Theor Chem Acc (2012) 131:1197
DOI 10.1007/s00214-012-1197-8

REGULAR ARTICLE

The polarizing forces of water

Revati Kumar · Thomas Keyes

Received: 2 May 2011 / Accepted: 9 September 2011 / Published online: 11 March 2012

Abstract A brief review of popular polarizable potentials for water, including both those parameterized to fit experimental properties, typically of the liquid, or electronic structure calculations on small clusters, is presented. The recently developed POLIR potential, which was parameterized to reproduce both ab initio calculations on clusters and the experimental liquid IR spectrum, is discussed, and some new results for both clusters and the liquid phase are shown, indicating its transferable nature.

Keywords Polarization · Vibrational spectra · Transferable potential

1 Introduction

Polarization can broadly be defined as the response of molecular electrostatic properties to an electric field, which may be applied externally or arise from the local environment, namely the surrounding molecules. The corresponding polarization energy and forces are nonadditive in nature, since the interaction between two molecules is influenced by the presence of other molecules. Most existing polarizable potentials [1–11] invoke dipole polarizable sites: In the presence of an electric field, a dipole is induced, which in turn changes the electric field elsewhere and interacts with the other charges, dipoles, induced dipoles, etc., of the system.

Published as part of the special collection of articles: From quantum mechanics to force fields: new methodologies for the classical simulation of complex systems.

R. Kumar · T. Keyes (✉)
Department of Chemistry, Boston Unviersity, Boston, MA, USA
e-mail: keyes@bu.edu

Note that even molecules without induced dipoles respond to an electric field by orienting their permanent dipoles, yielding a nonzero average system dipole. In this article, "polarization" denotes induced dipole polarization, which is our focus, not the "permanent dipole polarization" present in all models.

Polarization energies and forces are a class of many-body interactions. Consider three particles A, B, and C interacting with each other. The total "two-body" interaction is the sum of the interactions of A with B, B with C, and A with C. However, if the total interaction energy is not equal to the sum of these two-body energies, the remaining energy is referred to as the many-body energy (or in this case the three-body energy). Ab initio interaction energies are not pairwise additive, and the many-body interactions can be substantial. For example, ab initio calculations in water clusters have shown that while the two-body energy dominates and forms $\approx 80\%$ of the total energy, the many-body energies form the remaining $\approx 20\%$ [12].

Another indication of the importance of polarization in water is the change in dipole moment as one goes from the gas phase to the liquid. Gas-phase water molecules have a dipole moment of 1.85 D, while in the condensed phase, it goes up to an estimated range of 2.5–2.9 D [13, 14]. The increase is a result of polarization [15].

Polarization is not the only many-body interaction in nature, but it contributes significantly and, furthermore, provides a convenient framework to empirically include other many-body interactions in a force field [16, 17]. Furthermore, the short-range damping schemes [18] to be described below provide a treatment of classical charge penetration and an effective treatment of quantal exchange. Intramolecular charge transfer is treated via configuration-dependent charges, while intermolecular charge transfer is outside the scope of this work.

The earliest potentials developed for water were "effective" pair potentials like the SPC [19, 20] and TIPnP [21–26] families. These models have Coulomb interactions due to the partial charges, and Lennard–Jones type van der Waals interactions, both of which are two-body. However, by parameterizing with fits to experimental observables like the density and radial distribution functions of liquid water at around 300 K, they include, in an effective manner, the action of polarization. The resulting partial charges were found to give a higher dipole moment than the gas-phase monomer and closer to the value found in the liquid. While effective pair potentials do reasonably well for the liquid, they fail to describe water clusters [27, 28]. A number of them do poorly in reproducing the phases of ice and the melting temperature (unless they were parameterized to do so) [29, 30].

The ultimate goal is potentials that are transferable, that is, not limited to the conditions for which they were parameterized. Polarization, allowing many-body interactions and a dipole that varies with the environment, is a crucial element in this regard [31–33]. A nonpolarizable model that increases the monomer permanent dipole above the true monomer value to mimic the effect of polarization in the ambient liquid is obviously not transferable to small clusters [28], and probably not to high temperatures, since permanent dipole polarization is washed out by thermal agitation, while induced dipole polarization is not. Considerable effort has been directed to the development of polarizable force fields for water, because of its significance under diverse conditions and its evident signatures of polarization mentioned above, and because it acts as a test subject for general methodologies of force field development.

In this paper, we present a brief review of polarizable force fields for water, including the various techniques of implementing polarization. The manner of parameterization defines two main categories: They may be parameterized based either on experimental quantities associated with the condensed state, or on ab initio (electronic structure) calculations. The second half of the paper discusses some recent results using the flexible POLIR water potential recently developed in the Keyes group [10]. POLIR is a hybrid model in the sense that it was parameterized to both ab initio calculations on water clusters and the IR spectrum of the ambient liquid. POLIR does fairly well in predicting the properties of liquid water, despite having used no bulk information but the spectrum, and does remarkably well in reproducing additional spectroscopic properties that were not built in. In the original paper, Mankoo and Keyes showed that POLIR gets the HOH angle increase on going from the gas phase to the liquid. The calculated diffusion constant, radial distribution functions, and the dielectric constant of liquid water are reproduced reasonably well. In this paper, we further explore the properties of POLIR, both in clusters and in the liquid.

2 Theoretical methodology for polarization

In this section, we present a few of the methods used to describe polarization in force fields.

2.1 Point inducible dipoles

A brief description of the method of point inducible dipoles is provided by the following example. Consider a system of N water molecules with a dipole polarizability, α, on each oxygen atom. In addition, the H atoms and the O atoms have fixed charges, q_{H} and q_{O}, respectively, such that each molecule is neutral. The induced dipole moment, $\boldsymbol{\mu}_i$, on the O atom of molecule i is given by:

$$\boldsymbol{\mu}_i = \alpha \left[\mathbf{E}_i + \sum_{j \neq i} \mathbf{T}_{ij} \cdot \boldsymbol{\mu}_j \right], \tag{1}$$

where the two terms in the bracket are the field, $\mathbf{E}_i$, at the O atom of molecule i from the permanent charges excluding those on molecule i, and the field from other induced dipoles, where

$$\mathbf{E}_i = \sum_{j \neq i} \sum_{m=1,3} \frac{q_{j,m} \vec{r}_{i,1;j,m}}{r^3_{i,1;j,m}}. \tag{2}$$

The summation involves the atomic partial charges on molecule j at atomic site m, $q_{j,m}$, where $m = 1$ denotes the O-site on j, $m = 2, 3$ denotes the 2 H atoms on j, and $\vec{r}_{i,1;j,m}$ is the vector between the O-site on i and the atomic site m on j. Exclusion of intramolecular polarization by permanent charges is usual, but is not justified if one seeks to describe molecular vibrations. The dipole tensor $\mathbf{T}_{ij}$ is a 3×3 matrix whose elements are:

$$T^{\beta\gamma}_{ij} = \frac{3 r^{\beta}_{ij} r^{\gamma}_{ij}}{r^5_{ij}} - \frac{\delta_{\beta\gamma}}{r^3_{ij}}, \tag{3}$$

where β and γ denote the Cartesian components x, y, or z, $\delta_{\beta\gamma}$ is the Kronecker delta and $\vec{r}_{ij}$ refers to the vector between the O-sites of molecules i and j. The polarization energy is given by:

$$U_{\mathrm{pol}} = \sum_i \left[-\boldsymbol{\mu}_i \cdot \mathbf{E}_i - \sum_{j \neq i} [\boldsymbol{\mu}_i \cdot \mathbf{T}_{ij} \boldsymbol{\mu}_j] + \frac{1}{2\alpha} \boldsymbol{\mu}_i \cdot \boldsymbol{\mu}_i \right] \tag{4}$$

The induced dipoles are obtained from Eq. 1, and the straightforward solution involves matrix inversion. Unfortunately, this proves to be too expensive for most problems, and hence, iterative schemes are often used to obtain the induced dipoles and evaluate Eq. 4. One can also

use an extended Lagrangian formalism wherein the induced dipoles are treated as dynamical variables with an associated mass and are propagated in time [34].

The above equations can be generalized to include higher permanent moments (p) than charges alone. Eq 1 then takes the more general form,

$$\boldsymbol{\mu}_i = \alpha \cdot [\mathbf{E}^p + \mathbf{E}^{\text{ind}}]. \tag{5}$$

A problem with point dipoles is that, at short distances, the polarization energy diverges [18, 35]. For a diatomic parallel to the field, the "polarization catastrophe" occurs at an interatomic distance of $(4\alpha_1\ \alpha_2)^{1/6}$, where α_1 and α_2 are the polarizabilities of the two atoms/sites. In models with distributed atomic polarizabilities in which intramolecular induced dipole interactions are allowed, the distances can be short enough to cause this catastrophe. A number of methods have been proposed to overcome the problem, the most widely used of which is Thole's damping [18]. The electric field at site i, $\mathbf{E}_i$, and the elements of the dipole tensor, $\mathbf{T}_{ij}$, between sites i and j are given by

$$\mathbf{E}_i = \sum_{j \neq i} f_3(r_{ij}) \frac{q_j(r_{ij})\vec{r}_{ij}}{r_{ij}^3}, \tag{6}$$

where we note that the charge may be position dependent, and

$$T_{ij}^{\beta\gamma} = f_5(r_{ij}) \frac{3r_{ij}^{\beta} r_{ij}^{\gamma}}{r_{ij}^5} - f_3(r_{ij}) \frac{\delta_{\beta\gamma}}{r_{ij}^3}. \tag{7}$$

The damping functions, $f_3(r_{ij})$ and $f_5(r_{ij})$, are

$$f_3(r_{ij}) = 1 - \exp\left[-a\left[\frac{r_{ij}}{(\alpha_i\alpha_j)^{\frac{1}{6}}}\right]^b\right] \tag{8}$$

and

$$f_5(r_{ij}) = 1 - \left[1 + a\left[\frac{r_{ij}}{(\alpha_i\alpha_j)^{\frac{1}{6}}}\right]^b\right] \exp\left[-a\left[\frac{r_{ij}}{(\alpha_i\alpha_j)^{\frac{1}{6}}}\right]^b\right]. \tag{9}$$

The value of the exponent, b, is typically set to 3, although 4 and noninteger values have also been used [10, 36, 37]. The damping constant, a, was originally set to 0.5 by Thole, and a number of groups since then have used a as a parameter to be optimized [6, 7, 10, 11, 37, 38]. Different damping constants have been invoked for the dipole tensor and the electric field, and for intramolecular interactions and intermolecular interactions [7, 10, 37] Alternative damping functions have been proposed, including a linear Thole type and a Gaussian [39, 40].

2.2 Drude oscillator/charge-on-spring models

The underlying principle behind the Drude oscillator [41] and charge-on-spring [42, 43] models is that two charges of equal and opposite sign represent a dipole, which changes as the separation of the charges changes [44]. In the case of water, one of the charges ($-q_{\text{pol}}$) is fixed at the O-site, and the other charge (also called Drude particle, with $+q_{\text{pol}}$) is attached to the first charge via a harmonic spring (see Fig. 1), with an equilibrium separation of zero and a spring constant of k_{pol}. The position of the second charge is

$$\mathbf{r}_{\text{O}} + q_{\text{pol}}\mathbf{E}/k_{\text{pol}}. \tag{10}$$

The induced dipole is given by the product of the field-induced separation of the charges, q_{pol}, $\mathbf{E}/k_{\text{pol}}$, and the magnitude of the charge, q_{pol},

$$\boldsymbol{\mu} = q_{\text{pol}}^2\mathbf{E}/k_{\text{pol}}, \tag{11}$$

so the polarizability obeys $\alpha = q_{\text{pol}}^2\ /k_{\text{pol}}$. One difference between the charge-on-spring model of Yu et al. [42] and the Drude model (SWM4-DP) [41] is that the former has three sites, with the O atom carrying a charge q_{O} along with the induced dipole charge of $-q_{\text{pol}}$, whereas the latter has four sites, with the O atom carrying just the charge $-q_{\text{pol}}$, and the charge q_{O} of the oxygen shifted to an "M-site".

There are a number of ways that Eq. 11 can be solved to get the induced dipoles, for example, iterative methods as in the charge-on-spring implementation by the Yu et al. [42], extended Lagrangian type methods wherein the "Drude particle" is treated as a dynamical variable and propagated in time similar to the position vectors, etc [41].

2.3 Fluctuating charge models

In these models, the environment, through the electrostatic potential, is assumed to change the electronegativity of the atomic sites, and charge flow takes place in order to equalize the electronegativity [45]. The potential energy of a system with N charges is given by

$$U = \sum_{i=1}^{N} u_i + \sum_{i<j} \frac{q_i q_j}{r_{ij}} + U_{vdW}, \tag{12}$$

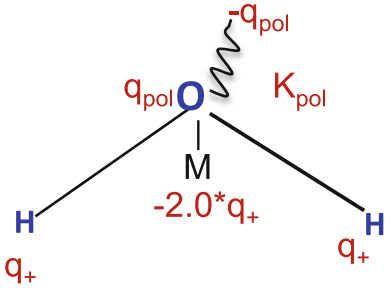

Fig. 1 A schematic diagram of the Drude oscillator model

where

$$u_i = u_0 + \chi_i q_i + \frac{1}{2} J_i q_i \tag{13}$$

is the energy of the creation of a partial charge, q_i. The derivative of U with respect to q_i gives the electronegativity per unit charge of atom i, and hence minimizing the energy with respect to the atomic charges, that is,

$$\frac{\delta U}{\delta q_i} = 0, \tag{14}$$

is equivalent to equalizing the electronegativities. Equation 14 gives rise to a set of coupled equations that can be solved either iteratively or, as in the Drude oscillator case, one can use an extended Lagrangian scheme wherein the charges are also considered to be dynamical variables. During the electronegativity equalization process, one can impose charge neutrality either on the molecule or simply on the entire system. In the latter case, charge transfer between molecules takes place, which in some case can be so high as to be physically unrealistic [44].

3 Types of polarizable models

One can divide polarizable models into two types, depending on whether they are primarily parameterized on experimental properties of the condensed phase, or on electronic structure calculations on water clusters. A brief description of some potentials belonging to these two categories is presented in the following two subsections.

3.1 Models parameterized to bulk experimental properties

Some of the earliest polarizable potentials, POL1 [1], RPOL [3], etc., were based on the work of Applequist et al. [46], wherein atomic polarizabilities were derived by fitting molecular polarizabilities to the experimental values. The Applequist-type models had both intra- and intermolecular polarization, but comparatively, small values of the atomic polarizabilities prevented a polarization catastrophe.

The POL1 model of Caldwell et al. used the Applequist values for the atomic polarizabilities and fit the remaining terms in the potential to get the liquid density and internal energy. The gas-phase molecular polarizability in POL1 is lower than the experimental value, and a modified version with the correct value, RPOL, was developed by Dang. The atomic polarizabilities were removed in the Dang-Chang [5] model and replaced by a single polarizability (with the gas-phase value of 1.44 Å) at a massless "M" site close to the O atom along the O–H bisector, which also carries the partial charge corresponding to the O atom. The partial charges and the position of the M-site were parameterized to reproduce the gas-phase dipole and quadrupole moments. Although the remaining parameters were essentially determined by fits to experimental properties of the liquid phase like the internal energy and diffusion constant, care was taken to obtain a reasonable description of cluster energies as well. However, this model consistently predicts lower three-body energies compared to the ab initio results for isomers of the water hexamer cluster [11].

Fluctuating charge as a mechanism of polarization was first introduced by Berne et al. in their SPC-FQ and TIP4P-FQ potentials [45], which are rigid with either the TIP4P or SPC geometry. An advantage of these models is that the force calculation is less time-consuming than the usual iteration to obtain the induced dipole, and the intermolecular interactions (apart from the van der Waals term) retained the Coulombic form with simple charge–charge interactions. Using the extended Lagrangian formalism, they were only 1.1 times slower than the corresponding fixed point charge models. Unfortunately, SPC-FQ and TIP4P-FQ have no out-of-plane polarizability [28].

The charge-on-spring models were parameterized to fit experimental quantities like the heat of vaporization and the density [42]. The SWM4-DP and SWM4-NDP (Drude) potentials were also parameterized to bulk experimental properties [41, 47]. The result is a good description of ambient liquid water, but not of clusters [28]. The SWM4-DP monomer has a much lower polarizability of 1.04 $Å^3$ as opposed to the experimental gas-phase value of 1.44 $Å^3$. However, it should be noted that the goal has been to efficiently introduce polarization into large biological simulations, for example, proteins, which are typically carried out at ambient conditions. The models now encompass not simply water, but other molecules like alkanes and aromatic compounds [48–50].

3.2 Ab initio-based models

Recent advances in electronic structure theory have made accurate high-level calculations on water clusters easily accessible, and force fields have been accordingly parameterized based upon two broadly different decomposition schemes of the ab initio energy:

1. Consider a system of n water molecules. For the sake of simplicity, let them be rigid, with the monomer energy denoted U_1. The energy of a dimer formed by molecules i and j is $U(ij)$, the energy of a trimer of molecules i, j, and k is $U(ijk)$, and so on. The ab initio interaction energy $\Delta U_n(1,2,3,\ldots,n)$ can be decomposed with a cumulant expansion [12, 51–53],

$$\Delta U_n = U(1,2,3,\ldots,n) - nU_1 = \sum_{i=1}^{n-1} \Delta U(ij) + \sum_{i=1}^{n-2} \sum_{j>i}^{n-1} \sum_{k>j}^{n} \Delta U(ijk) + \cdots \quad (15)$$

where $\Delta U(ij)$ and $\Delta U(ijk)$ are the two- and three-body energies,

$$\Delta U(ij) = U(ij) - 2U_1, \quad (16)$$

$$\Delta U(ijk) = U(ijk) - 3U_1 - (\Delta U(ij) + \Delta U(ik) + \Delta U(jk)). \quad (17)$$

This many-body decomposition scheme has been used to develop a number of water models. For example, in DPP [7] and DPP2 [11], the Thole damping of the polarizability was parameterized, so that the model recovers the three-body energy of water hexamers and the remaining terms were fit to the energies of a selection of water dimers (two-body energies).

2. One may also decompose the interaction energy into distinct physical contributions like the electrostatic component, the induction term, and the dispersion term. One of the earliest schemes is the Kitaura–Morokuma analysis [54]. Recently, the ALMO [55] and the SAPT [56] decompositions have been used to develop model potentials.

The two classes of decomposition method are not independent. For example, with SAPT, one can determine the two- and three-body contributions to the polarization energy, the exchange energy, and so on. These kinds of decompositions were used to parameterize, in part, the CC-pol [9] model, while DPP2 also used them to parameterize terms like the two-body dispersion energy.

One of the more widely used ab initio-based models is the AMOEBA potential [6]. It is flexible, with simple expressions for the zero-field monomer energy, including anharmonic contributions, for the bond stretching and bending terms, along with a term that couples the stretch and the bend. AMOEBA has permanent multipoles up to the quadrupole on each atom, obtained from distributed multipole analysis [57]. The atomic polarizabilities were taken from the work of Thole and, since intramolecular induced dipole–induced dipole interactions are allowed, Thole damping is included, with exponent $b = 3$. The damping constant, a, was determined by a fit to water cluster energies, and the van der Waal's interaction terms were fit so as to reproduce both the water dimer energies and some bulk properties like the liquid density.

Many of the models discussed so far like DPP, DPP2, CC-Pol, and TTM [58] are rigid. As one goes from the gas phase to the liquid, the HOH angle goes from 104.5° to around 107° [59]. However, most flexible potentials exhibit a decrease in the angle. In AMOEBA, the equilibrium angle in the monomer has been set to 108.5° to get agreement with liquid properties [6].

Accurate fits of the water monomer potential energy and dipole surface by Partridge and Schwenke [60], based on high-level ab initio calculations, proved to be a key ingredient in the development of accurate flexible members of the previously rigid TTM family by Burnham and Xantheas (TTM2-F [61]), Fanourgakis and Xantheas (revised TTM2-F [62] and TTM3-F [38]), and Burnham et al. (TTM4-F [37]). An important aspect of these models is their ability to reproduce the increase in the HOH angle upon condensation, as well as the vibrational spectra of water clusters, liquid water, and ice. The earlier flexible TTM potentials were not as successful as the later versions, namely TTM3-F and TTM4-F.

Interestingly, water in the gas phase dissociates to neutral radicals, which is the limiting case of the Partridge–Schwenke dipole surface [38]. However, in the liquid, the dissociation products are ions, and therefore, TTM3-F uses an appropriately modified dipole surface [38]. On the other hand, TTM4-F attempts to reproduce both the monomer dipole surface and the polarizability surface [37]. One should note that these models were parameterized using the results of electronic structure calculations and thus lack the effect of nuclear quantization, which could be included by the use of path integral methods like centroid molecular dynamics [63–65].

While most ab initio-based polarizable models include only dipole polarizabilities, the ASP potential of Millot and Stone includes both dipole and quadrupole polarizabilities [66]. It was parametrized to fit electronic structure calculations on both the monomer and the dimer and was later reparameterized (ASP-VRT) to fit spectroscopic data from vibrational-rotational-tunneling experiments [67].

The list of models mentioned in this section is by no means exhaustive. The broadly applicable algorithms for polarizable force field development, SIBFA (Sum of Interactions Between Fragments Ab initio computed) [68] and EFP (Effective Fragment Potential) [69], based on ab initio energy decomposition schemes, have associated water potentials. The GEM model of Piquemal et al. [70] is an extension of the SIBFA method wherein the atomic charge densities were fit to Gaussian s-type functions. As mentioned earlier, water acts as a "test subject" for development, and in that spirit, the SIBFA and the AMOEBA approaches have been extended to systems of biological interest [71, 72].

Although the polarizable potentials mentioned above can be around twenty times slower than simple point charge models in MD simulations [73], that price must be paid for a realistic description of systems with significant many-body effects, such as charged systems like excess electrons in water and heterogeneous systems like water in cavities [74–76].

3.3 POLIR potential

As mentioned in the introduction, POLIR is a hybrid water potential. It has permanent charges, permanent dipoles, and dipole polarizabilities on the O and H atoms. The charges depend on the internal geometry. If one labels one of the hydrogen atoms as H_1 and the other as H_2, then the charge on H_1 is given by

$$q_{H_1} = q^0 + c1 \cdot (r_{OH_1} + r_{OH_2} - 2 \cdot r_{OH}^{eq}) + c3 \cdot (r_{OH_1} - r_{OH_2}) \quad (18)$$

The charge on H_2 can be similarly written, and the charge on the O atom is given by $-(q_{H_1} + q_{H_2})$. The interaction terms are intermolecular charge–charge, inter- and intramolecular charge–permanent dipole and charge-induced dipole, dipole–dipole (which includes both permanent and induced dipoles), and intermolecular van der Waals, a function of the O–O distance. The charge–charge, charge–dipole, and dipole–dipole interactions are all damped using the Thole method. The zero-field monomer energy is given by the Partridge–Schwenke function, and therefore, in order to avoid double counting, the zero-field intramolecular charge–dipole and dipole–dipole energies are subtracted from the total energy.

POLIR takes nothing but the monomer potential energy function from Partridge–Schwenke. The charge, q^0, and all other elements of the dipole surface are determined in the fitting process and have no relation to PS. Note also that these parameters have a single value, they are not redetermined for different states of water.

The Thole damping constants, the constants $c1$ and $c3$ in the geometry-dependent charges, the polarizabilities, and the van der Waals terms are determined by fits to properties of the monomer (dipole surface, polarizability surface, etc.), dimer PES scan, and the pentamer minimum energy.

POLIR is constructed with the idea that polarization is so important for spectroscopy that the quality of the spectroscopic predictions is a good indicator of the quality of the overall description of polarization. Correspondingly, optimizing a potential for vibrational and intermolecular spectra is a good way to optimize the treatment of polarization. The equilibrium hydrogen charge, q^0, is determined primarily by fitting the O–H stretch region of the IR spectrum in the ambient liquid. Every time q^0 was varied, the potential parameters were refit to ensure that the potential reproduced the dimer PES, the monomer properties (e.g. the dipole moment) etc.

In the fit process, the correct frequency and absolute intensity occur simultaneously. Since the intensity is dominated by induced dipoles [77], the importance of polarization for the frequency shift is strongly suggested. Perhaps interestingly, the result is $q^0 = 0.42$, the value obtained [20] in the SPC/E potential, which attempts an effective treatment of polarization within a pairwise additive approach.

Note that POLIR is the only potential that includes the charge–dipole interaction on bonded OH atoms. It is difficult to see why this term should be negligible for vibrational spectroscopy. When an induced dipole changes, physics requires that its interaction with the charge on a bonded neighbor changes, which changes the vibrational frequency.

POLIR is designed to be used with classical simulations, in conjunction with the most simple, essential quantum corrections. In calculating the IR spectra, we use an harmonic intensity correction and the Berens–Wilson anharmonic frequency correction [78], which is a redshift of 184 cm^{-1} in the monomer, and, most encouragingly, not much different in the liquid and ionic solvation shell. Further details of the parameterization and the calculation of the IR spectra are given in Refs. [10, 33].

Because POLIR has been parameterized partially to the liquid-state experimental IR spectrum, and because of the anharmonic frequency correction, some effects of nuclear quantization have been implicitly taken into account. Therefore, an explicit treatment, for example, with centroid MD, would lead to some amount of double counting and does not fit with our approach. The internal energy of the ambient liquid using POLIR is -12.8 kcal/mol, and the experimental value is -9.9 kcal/mol [21]. The discrepancy could be due to nuclear quantization, but the agreement seems satisfactory for a quantity that was not incorporated in the parameterization. Although we have already demonstrated transferability for the potential energy of minimum energy configurations of clusters, this could be an issue for the average total energy.

3.3.1 Cluster properties

The original POLIR paper examined the IR harmonic spectra of a few water clusters [10]. Now, we explore in greater detail the energetic properties of an important water cluster—the hexamer; significant low-lying isomers are shown in Fig. 2. We compare the energies calculated with POLIR and other polarizable potentials with the ab initio energies (CCSD(T) [79] energies). Since some of these models are rigid, with the bond angles and bond lengths set to the gas-phase monomer, we took the ab initio clusters (from Ref. [11]) optimized with rigid monomer constraints. From the root mean square deviation in Table 1, it is clear that POLIR does very well in predicting the cluster energies (Fig. 3). We performed a many-body decomposition of the energies, as in Sect. 3.2, and the three-body energies (Fig. 4, Table 2) are once again quite impressive, all the more so given that the model was not parameterized to any hexamer properties.

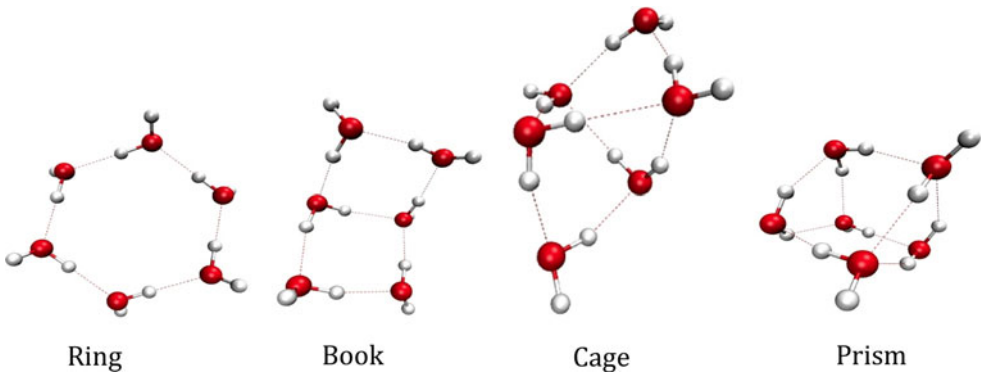

Fig. 2 The four isomers of the hexamer water cluster

Table 1 The root mean square deviation of the energies of the four isomers of the water hexamer cluster for the various models with respect to the ab initio CCSD(T) values

Model	RMSD with respect to CCSD(T)
DC	5.50
AMOEBA	0.47
TTM3-F	3.12
POLIR	0.39

The DC, AMOEBA, TTM3-F, and CCSD(T) results were taken from Ref. [11]

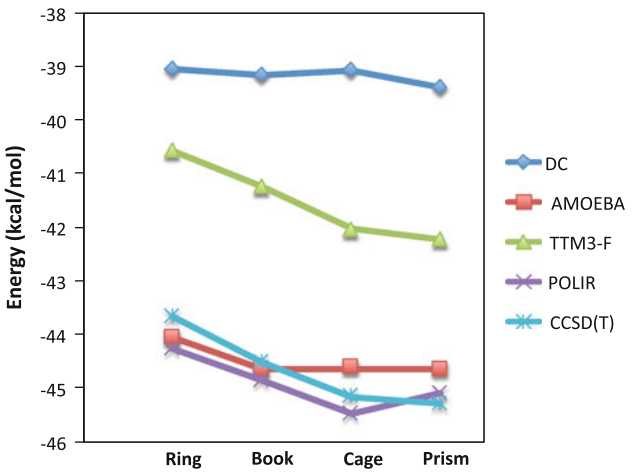

Fig. 3 The energies of the four isomers of the water hexamer cluster for the various models along with the ab initio CCSD(T) results. The DC, AMOEBA, TTM3-F, and CCSD(T) results were taken from Ref. [11]

3.3.2 Liquid-state properties

In order to calculate liquid-state properties, we performed MD simulations in the NVE ensemble at 300 K with periodic boundary conditions, using the Ewald summation [80] technique. The simulation box contained 128 water molecules at a density of 0.997 g/cc. The simulations were used to compare the rotational dynamics as well as the

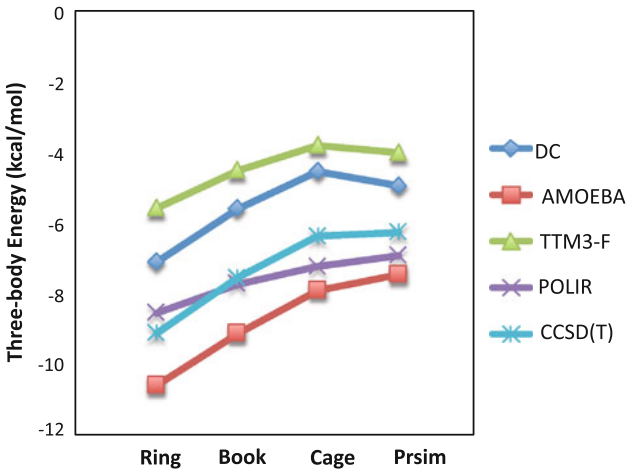

Fig. 4 The three-body energies of the four isomers of the water hexamer cluster for the various models along with the ab initio CCSD(T) results. The DC, AMOEBA, TTM3-F, and CCSD(T) results were taken from Ref. [11]

Table 2 The root mean square deviation of the three-body energies of the four isomers of the water hexamer cluster for the various models with respect to the ab initio CCSD(T) values

Model	RMSD with respect to CCSD(T)
DC	1.79
AMOEBA	1.43
TTM3-F	2.87
POLIR	0.61

The DC, AMOEBA, TTM3-F, and CCSD(T) results were taken from Ref. [11]

Raman spectra of POLIR with experimental results. We also examined the HOH angle distribution.

3.3.2.1 Rotational dynamics Mankoo and Keyes [10] obtained a diffusion constant of 2.4 cm^2/s, close to the experimental value of 2.3 cm^2/s [81]. Here, we continue the test of the dynamical aspects of POLIR. The rotational dynamics of water have been studied in great detail using both IR spectroscopy and NMR techniques [82–84]. These

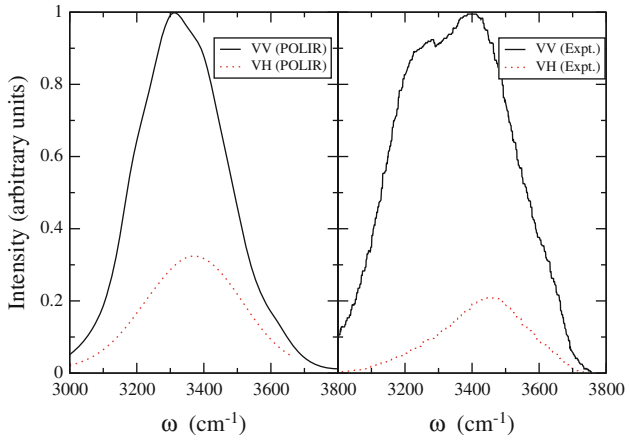

Fig. 5 The Raman spectra from POLIR and the experimental Raman spectra from Ref. [82]

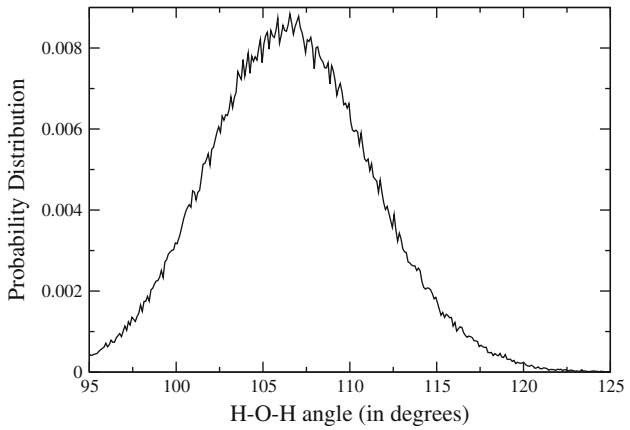

Fig. 6 The distribution of HOH angles in liquid water calculated with POLIR

experiments provide the characteristic rotational times for various vectors like the H–H vector, the O–H vector, and the vector normal to the plane of the molecule. The NMR rotational time for any unit vector, $\hat{u}$, is given by the integral (from 0 to ∞) of the correlation function, $C_{uu}(t)$, where

$$C_{uu}(t) = \langle P_2(\hat{u}(t) \cdot \hat{u}(0)) \rangle, \tag{19}$$

and $P_2(x)$ is the second Legendre function. We obtain a decay constant of 2.9 ps for both the H–H and O–H vectors, which compares well to the experimental values of 2.36 ps [82] and 2.4 ps [84], respectively. For the unit vector normal to the plane of the molecule, we find a characteristic time of 1.7 ps, while the experimental value is 1.8 ps [84].

3.3.2.2 Raman spectroscopy Raman spectra (Fig. 5) were calculated from the correlation functions of the appropriate elements of the polarizability tensor of the entire system [85],

$$I_{\mathrm{VV}}(\omega) \propto Q(\omega) \int_{-\infty}^{\infty} e^{-i\omega t} \langle \bar{\alpha}(0) \cdot \bar{\alpha}(t) + \frac{2}{15} Tr(\boldsymbol{\beta}(0) \cdot \boldsymbol{\beta}(t))) \rangle \mathrm{d}t \tag{20}$$

and

$$I_{\mathrm{VH}}(\omega) \propto Q(\omega) \int_{-\infty}^{\infty} e^{-i\omega t} \langle \frac{1}{10} Tr(\boldsymbol{\beta}(0) \cdot \boldsymbol{\beta}(t)) \rangle \mathrm{d}t \tag{21}$$

Here, $\bar{\alpha}$ is one-third the trace of the polarizability tensor, $\boldsymbol{\alpha}$, and $\boldsymbol{\beta}$ is the traceless anisotropic part.

$$\boldsymbol{\alpha} = \bar{\alpha} \boldsymbol{I} + \boldsymbol{\beta}. \tag{22}$$

In Fig. 5, we present the VV and VH spectra for POLIR in the O–H region, as well as the corresponding experimental spectra [86]. The calculated spectra are in reasonable agreement with experiment, although our VV line is somewhat too narrow. The Raman spectra were not used in the parameterization, and hence, this qualitative agreement is a true test of POLIR.

3.3.2.3 Bond angle POLIR gives an average bond angle of around 107°, in good agreement with experiment. We calculated the distribution of the bond angles (Fig. 6) and found it to be surprisingly broad, with significant populations ranging from as low as 95° to as high as 112°! This matches results from ab initio simulations [87] to the TTM2-F potential [59]. It is puzzling that rigid models do as well as they do in describing the liquid, given that they lack the high angular flexibility shown by "real" water. Examining the compensating effects in these rigid models might prove interesting.

4 Conclusion

For many years, theoretical and computational chemistry and physics focused on pair potentials, due to their tractability. It is now clear, however, that many-body energies and forces are not small corrections in water; they are extremely important. The need to go beyond pairwise additivity has been masked somewhat by the use of pair potentials optimized for a particular thermodynamic state, providing an effective treatment of many-body effects. However, such potentials are not transferable.

Polarization is both a real many-body effect and allows parameterization of other many-body effects. Consequently, considerable recent effort has been devoted to the development of polarizable potentials for water, with application to environments ranging from small clusters to the condensed phases. These models have been parameterized to fit either experimental properties or ab initio calculations on clusters, or in some cases both ("hybrid").

The importance of polarization is perhaps best seen by expanding the list of "test" properties beyond the usual pair distribution function, diffusion constant, etc., to spectroscopic properties. The vibrational IR intensity/molecule increases by a factor of 18× upon condensation [88], and the increase is due to polarization. The IR spectrum is seeing induced dipoles; that is, if the dipole is decomposed into its permanent and induced parts, the dipole correlation that determines the spectrum is dominated by the induced-induced term [77].

The POLIR potential was developed based on the idea that spectroscopic properties must enter the parameterization, as optimizing the spectra optimizes the treatment of polarization, which is important for everything else. POLIR has shown promising results for clusters, liquid water, solvated ions [33], and ice. While flexible, polarizable, models like POLIR are computationally challenging, the accurate treatment of the many-body polarization forces results in a transferable force field capable of reproducing spectroscopic properties.

Acknowledgments Acknowledgment is made to the donors of the American Chemical Society Petroleum Research Fund and to the National Science Foundation (grant CHE 0848427) for support of this research. The authors thank Prof. Brian Space for the digitized data of the experimental Raman spectrum and Prof. Kenneth Jordan for the structures of the isomers of the water hexamer cluster.

References

1. Caldwell J, Dang LX, Kollman PA (1990) J Am Chem Soc 112(25):9144–9147
2. Cieplak P, Kollman P, Lybrand T (1990) J Chem Phys 92(11):6755–6760
3. Dang LX (1992) J Chem Phys 97(4):2659–2660
4. Bernardo DN, Ding Y, Krogh-Jespersen K, Levy RM (1994) J Phys Chem 98(15):4180–4187
5. Dang LX, Chang T-M (1997) J Chem Phys 106:8149
6. Ren P, Ponder J (2003) J Phys Chem B 107:5933
7. Defusco A, Schofield DP, Jordan KD (2007) Mol Phys 105:2681
8. Li J, Zhou Z, Sadus RJ (2007) J Chem Phys 127(15):154509
9. Bukowski R, Szalewicz K, Groenenboom GC, van der Avoird A (2007) Science 315:1249
10. Mankoo PK, Keyes T (2008) J Chem Phys 129(3):034504
11. Kumar R, Wang F-F, Jenness GR, Jordan KD (2010) J Chem Phys 132(1):014309
12. Xantheas SS (2000) Chem Phys 258(2–3):225–231
13. Dyke TR, Muenter JS (1973) J Chem Phys 59(6):3125–3127
14. Gubskaya AV, Kusalik PG (2002) J Chem Phys 117(11):5290–5302
15. Adams D (1981) J Nat 293:447–449
16. Astrand PO, Linse P, Karlstroem G (1995) Chem Phys 191(1–3):195–202
17. Liu Y-P, Kim K, Berne BJ, Friesner RA, Rick SW (1998) J Chem Phys 108(12):4739–4755
18. Thole BT (1981) Chem Phys 59(3):341–350
19. Berendsen HJC, Postma WF, van Gunsteren WF, J, H (1981) Intermolecular forces. Reidel, Dordrecht
20. Berendsen HJC, Grigera JR, Straatsma TP (1987) J Phys Chem 91:6269
21. Jorgensen WL, Chandrasekhar J, Madura JD, Impey RW, Klein ML (1983) J Chem Phys 79:926
22. Mahoney MW, Jorgensen WL (2001) J Chem Phys 114:363
23. Horn HW, Swope WC, Pitera JW, Madura JD, Dick TJ, Hura GL, Head-Gordon T (2004) J Chem Phys 120(20):9665–9678
24. Rick SW (2004) J Chem Phys 120(13):6085–6093
25. Abascal JLF, Sanz E, Fernández RG, Vega C (2005) J Chem Phys 122(23):234511
26. Abascal JLF, Vega C (2005) J Chem Phys 123(23):234505
27. Kumar R, Christie RA, Jordan KD (2009) J Phys Chem B 113(13):4111–4118
28. Kiss PT, Baranyai A (2009) J Chem Phys 131(20):204310
29. Vega C, McBride C, Sanz E, Abascal JLF (2005) Phys Chem Chem Phys 7:1450–1456
30. Fernández RG, Abascal JLF, Vega C (2006) J Chem Phys 124(14):144506
31. Gregory JK, Clary DC, Liu K, Brown MG, Saykally RJ (1997) Science 275(5301):814–817
32. Wu JC, Piquemal J-P, Chaudret R, Reinhardt P, Ren P (2010) J Chem Theory Comput 6(7):2059–2070
33. Kumar R, Keyes T (2011) J Am Chem Soc 133:9441–9450
34. Sala J, Guàrdia E, Masia M (2010) J Chem Phys 133(23):234101
35. Stone AJ (1996) The theory of intermolecular forces. Clarendon Press, Oxford
36. Keyes T, Napoleon RL (2011) J Phys Chem B 115(3):522–531
37. Burnham CJ, Anick DJ, Mankoo PK, Reiter GF (2008) J Chem Phys 128(15):154519
38. Fanourgakis GS, Xantheas SS (2008) J Chem Phys 128(7):074506
39. van Duijnen PT, Swart M (1998) J Phys Chem A 102(14):2399–2407
40. Masia M, Probst M, Rey R (2005) J Chem Phys 123(16):164505
41. Lamoureux G, Alexander D, MacKerell J, Roux B (2003) J Chem Phys 119(10):5185–5197
42. Yu H, Hansson T, van Gunsteren WF (2003) J Chem Phys 118(1):221–234
43. Yu H, van Gunsteren WF (2004) J Chem Phys 121(19):9549–9564
44. Rick SW, Stuart S (2002) J rev Comput Chem 18:89–146
45. Rick SW, Stuart SJ, Berne BJ (1994) J Chem Phys 101(7):6141–6156
46. Applequist J, Carl JR, Fung K-K (1972) J Am Chem Soc 94(9):2952–2960
47. Lamoureux G, Harder E, Vorobyov IV, Roux B Jr, ADM (2006) Chem Phys Lett 418(1–3):245–249
48. Vorobyov IV, Anisimov VM, MacKerell AD (2005) J Phys Chem B 109(40):18988–18999
49. Lopes PEM, Lamoureux G, Roux B, MacKerell AD (2007) J Phys Chem B 111(11):2873–2885
50. Baker CM, Lopes PEM, Zhu X, Roux B, MacKerell AD (2010) J Chem Theor Comput 6(4):1181–1198
51. Kumar R, Skinner JL (2008) J Phys Chem B 112(28):8311–8318
52. Harkins D, Moskowitz J, Stillinger FH (1970) J Chem Phys 53:4544
53. Xantheas S (1994) J Chem Phys 100:7523
54. Kitaura K, Morokuma K (1976) Int J Quantum Chem 10(2):325–340
55. Khaliullin RZ, Cobar EA, Lochan RC, Bell AT, Head-Gordon M (2007) J Phys Chem A 111(36):8753–8765
56. Jeziorski B, Moszyński R, Szalewicz K (1994) Chem Rev 94:1887–1930
57. Stone AJ, Alderton M (1985) Mol Phys 56:1047
58. Burnham CJ, Xantheas SS (2002) J Chem Phys 116:1500
59. Fanourgakis GS, Xantheas SS (2006) J Chem Phys 124(17):174504

60. Partridge H, Schwenke DW (1997) J Chem Phys 106(11):4618–4639
61. Burnham CJ, Xantheas SS (2002) J Chem Phys 116(12):5115–5124
62. Fanourgakis G, Xantheas S (2006) J Phys Chem A 110(11):4100–4106
63. Cao J, Voth GA (1993) J Chem Phys 99(12):10070–10073
64. Cao J, Voth GA (1994) J Chem Phys 100(7):5093–5105
65. Cao J, Voth GA (1994) J Chem Phys 100(7):5106–5117
66. Millot C, Stone A (1992) Mol Phys 77:439–462(24)
67. Goldman N, Leforestier C, Saykally R (2005) J Philos Trans A Math Phys Eng Sci 363(1827):493–508
68. Piquemal J-P, Chelli R, Procacci P, Gresh N (2007) J Phys Chem A 111(33):8170–8176
69. Day PN, Jensen JH, Gordon MS, Webb SP, Stevens WJ, Krauss M, Garmer D, Basch H, Cohen D (1996) J Chem Phys 105(5):1968–1986
70. Piquemal J-P, Cisneros GA, Reinhardt P, Gresh N, Darden TA (2006) J Chem Phys 124(10):104101
71. Ponder JW, Wu C, Ren P, Pande VS, Chodera JD, Schnieders MJ, Haque I, Mobley DL, Lambrecht DS, DiStasio RA, Head-Gordon M, Clark GNI, Johnson ME, Head-Gordon T (2010) J Phys Chem B 114(8):2549–2564
72. Roux C, Bhatt F, Foret J, de Courcy B, Gresh N, Piquemal J-P, Jeffery CJ, Salmon L (2011) Proteins Struct Funct Bioinf 79(1):203–220
73. Fanourgakis G, Tipparaju V, Nieplocha J, Xantheas S (2007) Theor Chem Acc 117:73–84
74. Jorgensen WL, McDonald NA, Selmi M, Rablen PR (1995) J Am Chem Soc 117(47):11809–11810
75. Sommerfeld T, DeFusco A, Jordan KD (2008) J Phys Chem A 112(44):11021–11035
76. Bucher D, Rothlisberger U (2010) J Gen Physiol 135(6):549–554
77. Ahlborn H, Xingdong J, Space B, Moore P (1999) J Chem Phys 111:10622
78. Berens P, Wilson KR (1981) J Chem Phys 74:4872
79. Raghavachari K, Trucks GW, Pople JA, Head-Gordon M (1989) Chem Phys Lett 157(6):479–483
80. Smith W (1998) CCP5 Newslett 46:18
81. Krynicki K, Green CD, Sawyer DW (1978) Faraday Discuss Chem Soc 66:199–208
82. Jonas J, DeFries T, Wilbur DJ (1976) J Chem Phys 65(2):582–588
83. Tan H-S, Piletic IR, Fayer MD (2005) J Chem Phys 122(17):174501
84. Ropp J, Lawrence C, Farrar TC, Skinner JL (2001) J Am Chem Soc 123(33):8047–8052
85. McQuarrie DA (2000) Statistical mechanics. University Science Books, Mill Valley
86. Hare D, Sorensen C (1990) J Chem Phys 93:25–33
87. Cristobal A, Kyoungrim B, Jiali G (1998) In: Combined quantum mechanical and molecular mechanical methods, chap 4. American Chemical Society, Washington, DC, pp 35–49
88. Bertie JE, Ahmed MK, Eysel HH (1989) J Phys Chem 93(6):2210–2218